Eulerian-Lagrangian Method of Cells Based on Localized Adjoint Method

G. Herrera
Department of Engineering and Mathematics, University of Vermont, Burlington, Vermont 05405

I. Herrera
Institute of Geophysics, National University of Mexico, Apartado Postal 22-582, Mexico D.F. 14000, Mexico

Received 15 January 1993; revised manuscript received 28 June 1993

The localized adjoint method, when applied using an Eulerian-Lagrangian frame, has been quite successful in treating advection-dominated transport. The resulting methodology is known as ELLAM. In previous work, bilinear functions were used as test functions. In this paper, local constant functions are used instead, leading to procedures which are appealing because, in addition to other advantages of ELLAM methods, they ensure local mass conservation, are easy to apply and can be combined without difficulty with existing solute-transport codes which are based on finite volumes. In addition, the procedures for deriving the algorithms presented here are used as an illustration of a general methodology for treating numerically partial differential equations, which is advocated by the authors. Such methodology consists in identifying the information about the sought solution which is contained in the approximate one and then using this insight to choose the interpolation procedure to be applied.

I. INTRODUCTION

The numerical solution of the advective-diffusive transport equation is a problem of great importance because many problems in science and engineering involve such a mathematical model. When dissipation dominates, most numerical methods produce adequate results. However, when the process is advection dominated the problem is especially difficult and most numerical schemes exhibit either nonphysical oscillations or excessive numerical dissipation, or both. Upstream weighting, which often is used to address these problems, frequently generates artificial dissipation whose magnitude is of the order of the size of the grid spacing.

Two important classes of numerical schemes that have been used to overcome the difficulties in advection-dominated problems are based on applying localized adjoint methods (LAM) [1–8]. They are derived from two approaches: optimal spatial methods (OSM) and characteristic methods (CM). In the first one of these approaches, a Eulerian frame of reference (fixed grid) is employed to apply the LAM methodology [9]. These

Numerical Methods for Partial Differential Equations, 10, 205–223 (1994)
 CCC 0749-159X/94/020205-19

techniques yield methods that are optimal in space, in the sense that in one-dimensional problems the space solution is exact at the nodes, in the constant-coefficient case, and highly accurate in the nonconstant-coefficient case [6, 7]. However, they introduce very large time-truncation errors.

In the second approach, a Lagrangian (characteristic) frame of reference is employed to apply the LAM methodology, leading to what is called the Eulerian-Lagrangian localized adjoint method (ELLAM) [10–13]. Like characteristic methods [14–20], in general, this method has the advantage that Courant number restrictions of purely Eulerian methods are removed to a large extent. However, they present several important additional advantages. Characteristic methods, in general, have three kinds of limitations: inability to rigorously treat boundary fluxes when characteristics intersect inflow or outflow boundaries. This is reflected in their inability to ensure mass conservation and the introduction of numerical dispersion for some methods, due to low-order interpolation or integration [21]. In contrast to other characteristic methods, ELLAM permits a systematic incorporation of boundary conditions and yields mass conservative schemes [10, 12].

There are several ways in which ELLAM can be implemented, depending on the test functions used. The first that was applied is a finite-element formulation which used, as test functions, bilinear functions that were advected with the velocity of the fluid [10]. In this paper, we present an alternative to such an approach, in which the test functions are piecewise constant, and are advected with the transport velocity of the problem. We call such a method ELLAM cells, to distinguish it from the previous one [10], which we call bilinear ELLAM (BELLAM). The procedure we propose has the advantages of ELLAM methods, described above, but in addition it ensures local mass conservation and yields algorithms that are more convenient for existing solute-transport codes which are based on finite volumes. Also, the simplicity of the implementation of the method is appealing.

It must be mentioned that we are aware of another procedure in which similar (but different, as is explained later on) test functions are used [22]. However, the point of view and the manner in which the schemes are implemented are so different in the two methods that they are clearly distinct. Some of these differences and the relative merits of these approaches will be discussed in detail in several sections of the article. Here, we only cite a few.

To distinguish between these two methods, we will call FVELLAM the method introduced in [22], as suggested in that paper, and will reserve the term ELLAM cells for the method we propose in the present article. Typical finite-volume methods lump the storage integrals and assume that the concentration is piecewise constant within each cell. However, it was found in [22], and we have corroborated, that such a procedure introduces unacceptable levels of numerical dispersion. To improve the situation, in FVELLAM a linear variation (actually, bilinear: linear on each side of the cell center, separately) on each cell was assumed. In passing, we comment that this is quite similar to a finite-element approach, since such an assumption is equivalent to using a bilinear basis function.

On the other hand, the point of view adopted in this article, which is explained in the following sections, advocates identifying first the information about the exact solution contained in the approximate one and then processing it, in the most efficient manner that is possible, without prejudging its shape. This allows the derivation of more precise approximations, because assuming the shape of the solution unduly restricts the accuracy of the algorithms that can be obtained. This was corroborated by the fact that many of the numerical difficulties that were encountered when developing FVELLAM [22] did not occur in the development of ELLAM cells.

Apparently, most of the other differences between the two methods derive from this one and were due to *ad hoc* modifications that were introduced in FVELLAM, in order to improve difficulties that were not encountered in ELLAM cells. To mention just one, in spite of the fact that initially in FVELLAM, it was intended that piecewise constant functions be used as test functions, they were modified to be what the authors call "approximate test functions," which are nonconstant [22]. In contrast, in ELLAM cells the use of test functions which are piecewise constant did not produce any numerical difficulty. On the contrary, the numerical formulation is simpler than that of bilinear ELLAM.

II. BACKGROUND

In previous work [4, 11], it has been pointed out that in the construction of approximate solutions two important processes occur: (i) gathering information about the sought solution, and (ii) interpolating or, more generally, processing such information. These two processes are distinct, although in many numerical methods they are not differentiated clearly. The information about the exact solution that is gathered is determined mainly by the weighting functions used. Since this information does not determine uniquely the sought solution, some processing of it is required in order to fill the gaps of information and exhibit at the end a unique approximate solution.

Different methods of solution follow different strategies for carrying out this process of extending the information that is available (interpolation, extrapolation, or both). For example, in finite-element methods some basis functions are chosen and the approximate solution is assumed to be a superposition of such functions. In this case, the information about the exact solution which is gathered by the weighting functions is interpolated in a manner which is determined by the family of basis functions chosen.

Clearly, it is disadvantageous to carry out the process of extending the information blindly, not knowing what is the actual information that is available. However, this is what is usually done. On the contrary, it is advantageous to make use of the insight gained when the available information has been identified, since the selection of the best procedure for extending such information is strongly dependent on the information that is at hand.

Due to these facts, in recent works the authors [4, 11–13] have advocated an approach for developing numerical methods in which the processes (i) and (ii) are clearly separated, the information about the sought solution that is at hand is identified, and then the process of extending it is based on that knowledge.

The procedure used for deriving the algorithms presented in this article is an illustration of such methodology. Using Herrera's algebraic theory of boundary-value problems [4–6] (some background material for the development of this theory is presented in [23] and additional results of the theory are given in [24] and [25]), which permits localizing the adjoint, the information contained in the approximate solution is identified and analyzed [1, 11]. This is what should be properly called the localized adjoint method. Then, depending on the information that is identified, interpolation procedures suitable for handling it efficiently are selected and applied. In most cases the introduction of basis functions is not required and, even more, their use is frequently inconvenient, such as for the problem treated in this article. These points will be discussed further, later on.

An important point to be made is that the use of the algebraic theory for the analysis of the information has clear advantages over other options, such as the standard theory of distributions, because of at least two reasons: the use of the algebraic theory permits

the localization of the adjoint and the simultaneous use of discontinuous trial and test functions is feasible.

III. METHOD FOR ANALYZING THE INFORMATION

As mentioned previously, a convenient manner of carrying out the analysis of the information contained in approximate solutions is by application of Herrera's algebraic theory of boundary-value problems [5, 6, 23, 24]. A special feature is that the analysis is carried out using exclusively simple inner products which are defined locally. The theory implies a kind of operator extension which differs from the theory of distributions [25].

The main result required is a Green formula for functions with jump discontinuities (Green-Herrera formula), which is explained in this section in a brief manner. In its original form it was presented in [5, 6, 24], but the interested reader will find detailed and updated expositions, for partial differential equations and systems of such equations, in [1] and [11]. In some specific applications, it is feasible to derive the results which are needed in an *ad hoc* manner, instead of deriving them from the general formulas of the theory (see, for example, [10]). However, the framework of the general theory supplies the guidelines that permit understanding more thoroughly the methodology of analysis, which is applicable to a great variety of problems, including systems of differential equations [11].

Consider functions defined in a region Ω (possibly space-time), which may have jump discontinuities across some internal boundary Σ. In applications to finite-element methods, Σ could be the union of all the interelement boundaries. The general boundary-value problem treated by the theory is one with prescribed jumps across Σ. The differential equation is

$$\mathcal{L}u = f_\Omega \quad \text{in } \Omega\,.$$

Certain boundary and jump conditions are specified on the boundary $\partial\Omega$ of Ω and on Σ, respectively. When Ω is a space-time region, initial conditions may be thought as part of the boundary conditions, since they apply in part of the boundary of Ω.

Given a differential operator $\mathcal{L}$ and its adjoint $\mathcal{L}^*$, the Green-Herrera formula is

$$\int_\Omega w\mathcal{L}u\,dx - \int_{\partial\Omega} \mathcal{B}(u,w)\,dx - \int_\Sigma \mathcal{J}(u,w)\,dx = \int_\Omega u\mathcal{L}^* w\,dx - \int_{\partial\Omega} \mathcal{C}^*(u,w)\,dx - \int_\Sigma \mathcal{K}^*(u,w)\,dx\,, \tag{3.2}$$

where $\mathcal{B}$ and $\mathcal{J}$ are bilinear functions of u and w, defined pointwise, while $\mathcal{C}^*$ and $\mathcal{K}^*$ are the transposes of $\mathcal{C}$ and $\mathcal{K}$, respectively, which are also bilinear in u and w.

Equation (3.2) can be obtained applying successive integration by parts. However, a more systematic way, which permits exhibiting the framework that can be used in a very general class of problems, is presented here. It starts from the definition of formal adjoint, which requires that $\mathcal{L}$ and $\mathcal{L}^*$ satisfy

$$w\mathcal{L}u - u\mathcal{L}^* w = \nabla \cdot \{\underline{\mathcal{D}}(u,w)\} \tag{3.3}$$

for a suitable vector-valued bilinear function $\underline{\mathcal{D}}(u,w)$. Integration over Ω of Eq. (3.3) and application of generalized divergence theorem [26] yield:

$$\int_\Omega \{w\mathcal{L}u - u\mathcal{L}^* w\}\, dx = \int_{\partial\Omega} \mathcal{R}_\partial(u,w)\, dx + \int_\Sigma \mathcal{R}_\Sigma(u,w)\, dx\,,$$

where the bilinear functions $\mathcal{R}_\partial$ and $\mathcal{R}_\Sigma$ are defined on $\partial\Omega$ and Σ, respectively, by

$$\mathcal{R}_\partial(u,w) = \underline{\mathcal{D}}(u,w) \cdot \underline{n}$$

and

$$\mathcal{R}_\Sigma(u,w) = -[\,\underline{\mathcal{D}}(u,w)] \cdot \underline{n}\,. \tag{3.5}$$

Here, the square brackets stand for the "jumps" across Σ of the function contained inside, i.e., limit on the positive side minus limit on the negative side. The positive side of Σ is chosen arbitrarily and then the unit normal vector $\underline{n}$ is taken pointing towards the positive side of Σ. Observe that generally $\mathcal{L}u$ will not be defined on Σ, since u and its derivatives may be discontinuous. Thus, in the theory, it is understood that integrals over Ω are carried out excluding Σ. Consequently, differential operators must be always understood in an elementary sense and not in a distributional sense.

In the general theory of partial differential equations, Green's formulas are used extensively. For the construction of such formulas it is standard to introduce a decomposition of the bilinear function $\mathcal{R}_\partial$. Indicating transposes of bilinear forms by means of a star, the general form of such decomposition is

$$\mathcal{R}_\partial(u,w) \equiv \underline{\mathcal{D}}(u,w) \cdot \underline{n} = \mathcal{B}(u,w) - \mathcal{C}^*(u,w)\,, \tag{3.6}$$

where $\mathcal{B}(u,w)$ and $\mathcal{C}(w,u) = \mathcal{C}^*(u,w)$ are two bilinear functions. When considering initial-boundary-value problems, the definitions of these bilinear forms depend on the type of boundary and initial conditions to be prescribed. They are chosen satisfying the requirement that for any u that fulfills the prescribed boundary and initial conditions, $\mathcal{B}(u,w)$ is a well-defined linear function of w, independent of the particular choice of u. This linear function will be denoted by g_∂ [thus its value for any given function w will be $g_\partial(w)$], and the boundary conditions can be specified by requiring that $\mathcal{B}(u,w) = g_\partial(w)$ for every test function w.

The linear function $\mathcal{C}^*(u,\cdot)$, on the other hand, cannot be evaluated in terms of the prescribed boundary values, but it also depends exclusively on certain boundary values of u (the "complementary boundary values"). Generally, such boundary values can only be evaluated after the initial-boundary-value problem has been solved.

In a similar fashion, convenient formulations of boundary-value problems with prescribed jumps require constructing Green's formulas in discontinuous fields. The Green-Herrera formula is obtained, introducing the general decomposition

$$\mathcal{R}_\Sigma(u,w) = \mathcal{J}(u,w) - \mathcal{K}^*(u,w) \tag{3.7}$$

pagegoal = 48pc

of the bilinear function $\mathcal{R}_\Sigma(u,w)$. This has been done in general for differential operators whose coefficients may be discontinuous [5]. However, the decomposition is especially easy to obtain when the coefficients are continuous, since for this case it stems from the algebraic identity

$$[\,\underline{\mathcal{D}}(u,w)] = \underline{\mathcal{D}}([u],\dot{w}) + \underline{\mathcal{D}}(\dot{u},[w])$$

if $\mathcal{J}$ and $\mathcal{K}^*$ are defined by

$$\mathcal{J}(u,w) = -\underline{\mathcal{D}}([u],\dot{w}) \quad \underline{n}\,.$$

$$\mathcal{K}^*(u,w) = \mathcal{K}(w,u) = \underline{\mathcal{D}}(\dot{u},[w]) \cdot \underline{n}. \tag{3.9b}$$

$$[u] = u_+ - u_-, \quad \dot{u} = (u_+ + u_-)/2. \tag{3.10}$$

An important property of the bilinear function $\mathcal{J}(u,w)$ is that, when the jump of u is specified, it defines a unique linear function of w, which is independent of the particular choice of u. When considering initial-boundary-value problems with prescribed jumps, the linear function defined by the prescribed jumps in this manner will be denoted by j_Σ [thus its value for any given function w will be $j_\Sigma(w)$] and the jump conditions at any point of Σ can be specified by means of the equation $\mathcal{J}(u,w) = j_\Sigma(w)$. If the sought solution is required to be smooth, one would usually have $j_\Sigma(w) \equiv 0$.

In problems with prescribed jumps, the linear functional value problem has been solved and certain information about the average of the solution and its derivatives on Σ is known. Such information is called the "generalized averages."

A weak formulation of the boundary-value problem with prescribed jumps is

$$\int_\Omega w\mathcal{L}u\,dx - \int_{\partial\Omega} \mathcal{B}(u,w)\,dx - \int_\Sigma \mathcal{J}(u,w)\,dx = \int_\Omega w f_\Omega\,dx - \int_{\partial\Omega} g_\partial(w)\,dx - \int_\Sigma j_\Sigma(w)\,dx. \tag{3.11a}$$

However, this weak formulation is equivalent to

$$\int_\Omega u\mathcal{L}^*w\,dx - \int_{\partial\Omega} \mathcal{C}^*(u,w)\,dx - \int_\Sigma \mathcal{K}^*(u,w)\,dx = \int_\Omega w f_\Omega\,dx - \int_{\partial\Omega} g_\partial(w)\,dx - \int_\Sigma j_\Sigma(w)\,dx \tag{3.11b}$$

by virtue of Eq. (3.2). Equation (3.11a) is the variational formulation in terms of the data of the problem, while (3.11b), is the variational formulation in *terms of the sought information.*

The analysis of the information contained in approximate solutions is based in the following observations. When the method of weighted residuals is applied, using a system of weighting functions $\{w^1,\ldots,w^N\}$, an approximate solution satisfies

$$\int_\Omega \hat{u}\mathcal{L}^*w^\alpha\,dx - \int_{\partial\Omega} \mathcal{C}^*(\hat{u},w^\alpha)\,dx - \int_\Sigma \mathcal{K}^*(\hat{u},w^\alpha)\,dx = \int_\Omega w^\alpha f_\Omega\,dx - \int_{\partial\Omega} g_\partial(w^\alpha)\,dx - \int_\Sigma j_\Sigma(w^\alpha)\,dx, \quad \alpha = 1,\ldots,N. \tag{3.12}$$

Taking into account that Eq. (3.12) is also satisfied by the exact solution, it is seen that

$$\int_\Omega (\hat{u}-u)\mathcal{L}^*w^\alpha\,dx - \int_{\partial\Omega} \mathcal{C}^*(\hat{u}-u,w^\alpha)\,dx - \int_\Sigma \mathcal{K}^*(\hat{u}-u,w^\alpha)\,dx = 0. \tag{3.13}$$

Equation (3.13) is the basis for analyzing the information contained in approximate solutions. The term $\int_\Omega(\hat{u}-u)\mathcal{L}^*w^\alpha\,dx$ gives the information about the exact solution u in the interior of the region of definition of the problem Ω; the term $\int_{\partial\Omega} \mathcal{C}^*(\hat{u}-u,w^\alpha)\,dx$ gives the information about the complementary boundary values on $\partial\Omega$; and the term $\int_\Sigma \mathcal{K}^*(\hat{u}-u,w^\alpha)\,dx$ gives the information about the generalized averages in the interelement boundaries Σ.

Consider now the one-dimensional transient advection-diffusion equation, in conservative form:

$$\mathcal{L}u \equiv \frac{\partial u}{\partial} - \frac{\partial}{\partial x}\left(D\frac{\partial u}{\partial x} - Vu\right) = f_\Omega \tag{3.14}$$

subject to initial conditions

$$u(x,0) = u_0(x) \tag{3.15}$$

and suitable boundary and jump conditions, which for the time being are left unspecified. In addition, for convenience, it will be assumed that $V \geq 0$ everywhere. In space, the interval of definition of the problem will be $[0,l] = \Omega_x$. Observe that in this case the adjoint operator is given by

$$\mathcal{L}^* w \equiv -\frac{\partial w}{\partial t} - \frac{\partial}{\partial x}\left(D\frac{\partial w}{\partial x}\right) - V\frac{\partial w}{\partial x} \tag{3.16}$$

Then

$$w\mathcal{L}u - u\mathcal{L}^* w = \nabla \cdot \{\underline{\mathcal{D}}(u,w)\}$$

with

$$\underline{\mathcal{D}}(u,w) = \left\{u\left(D\frac{\partial w}{\partial x} + Vw\right) - wD\frac{\partial u}{\partial x}, uw\right\}. \tag{3.18}$$

In Eq. (3.17) the divergence is understood to be in space-time.

When constructing a solution of this problem step by step in time, it is convenient to decompose the time into subintervals. Let $[t_n, t_{n+1}]$ be one such subinterval (Fig. 1); then assuming that the solution at t_n has already been obtained, a procedure for constructing it at t_{n+1} is required. This is the problem we address in what follows. The region of definition of such problem is $\Omega = \Omega_x \times [t_n, t_{n+1}]$ and the initial conditions of Eq. (3.15) have to be replaced by

$$u(x,t_n) = u^n(x), \tag{3.19}$$

where the function $u^n(x)$ corresponds to the values of the solution at time t_n, which by assumption have been previously obtained.

A partition $\{x_1, x_{3/2}, x_{5/2}, \ldots, x_{E-1/2}, x_E\}$ into E subintervals of the interval $[0,l]$ is introduced, for which $x_1 = 0$ and $x_E = l$. The points

$$x_i = (x_{i-1/2} + x_{i+1/2})/2, \quad i = 2, \ldots, E-1, \tag{3.20}$$

will be referred to as the "cell centers." Notice that x_1 and x_E are boundary points of $[0,l]$ and they are not midpoints of any of the subintervals. The partition will be called "uniform" when $h_i = x_{i+1/2} - x_{i-1/2} = h$ is independent of i, for $i = 2, \ldots, E-1$, and in addition, $x_{3/2} - x_1 = x_E - x_{E-1/2} = h/2$.

The region Ω is decomposed into a collection of subregions $\Omega_1, \ldots, \Omega_E$, limited by space-time curves $\Sigma_{i+1/2}, i = 1, \ldots, E-1$, each one of them passing through $x_{i+1/2}$ at time t_{n+1}, as shown in Fig. 1. It will be assumed that discontinuities may occur on these lines exclusively and we write

$$\Sigma = \bigcup_{i=1}^{E-1} \Sigma_i .$$

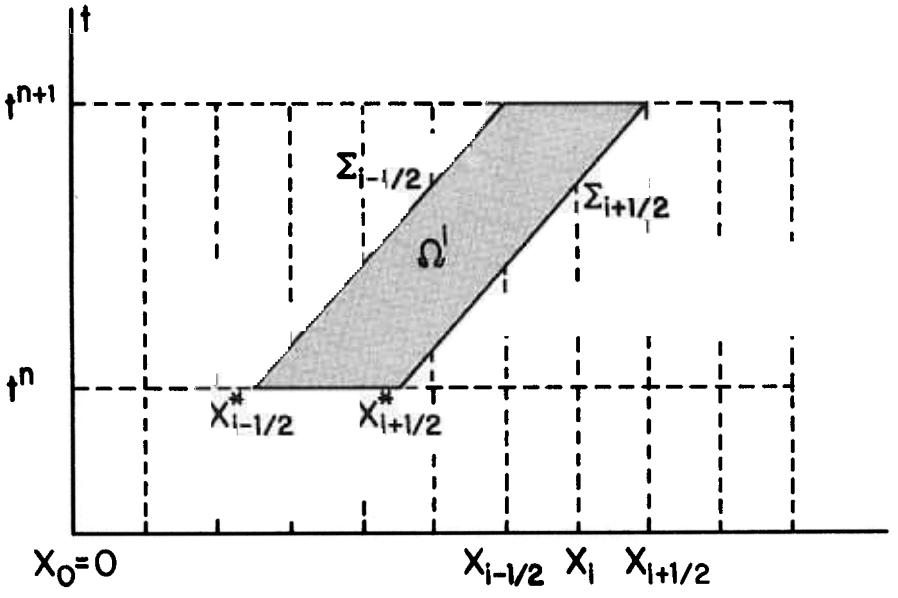

FIG. 1. Partition of the region Ω.

The velocity of propagation of these lines of discontinuity is denoted by V_Σ. In particular, when $V_\Sigma = V$, such a line is a characteristic curve.

The bilinear function $\mathcal{K}(w,u)$ is associated with the values of u and its first-order derivative on Σ, and can be written as

$$\mathcal{K}(w,u) = \mathcal{K}^0(w,u) + \mathcal{K}^1(w,u), \tag{3.21}$$

where the two bilinear functions $\mathcal{K}^0(w,u)$ and $\mathcal{K}^1(w,u)$ are defined by

$$\mathcal{K}^0(w,u) = (1 + V_\Sigma^2)^{-1/2}\dot{u}\left\{\left[D\frac{\partial w}{\partial x}\right] + (V - V_\Sigma)[w]\right\}, \tag{3.22a}$$

$$\mathcal{K}^1(w,u) = -(1 + V_\Sigma^2)^{-1/2}[w]D\frac{\partial u}{\partial x}. \tag{3.22b}$$

The remaining functions can be defined similarly and the details have been given in [11].

IV. ELLAM CELLS

In this section, we address the problem of solving the advection-diffusion initial-boundary-value problem formulated in Sec. III, taking $f_\Omega \equiv 0$. The sought solution will be required to be smooth. More precisely, it will be assumed that u and its first spatial derivative are continuous across Σ.

A special notation will be used for the characteristic curves of the first-order differential equation that is obtained setting $D \equiv 0$ in (3.14). Thus, let the function $X(t;\hat{x},\hat{t})$ be such that, for every $\hat{x}$ and $\hat{t}$, it satisfies

$$\frac{\partial X}{\partial t}(t;\hat{x},\hat{t}) = V(X(t;\hat{x},\hat{t}),t) \tag{4.1a}$$

subject to the condition that

$$X(t;\hat{x},\hat{t}) = \hat{x} \tag{4.1b}$$

Then the graph

$$x = X(t;\hat{x},\hat{t}) \tag{4.2}$$

is the characteristic curve which passes through the point $(\hat{x},\hat{t})$. In particular, for the characteristic passing through $x_{i+1/2}$ at time t_{n+1}, the notation $\Sigma_{i+1/2}$ will be used. This is given by

$$x = X(t;x_{i+1/2},t_{n+1}). \tag{4.3}$$

The position of $\Sigma_{i+1/2}$ at time t_n will be denoted by $x^*_{i+1/2}$ (Fig. 1) and it is given by

$$x^*_{i+1/2} = X(t;x_{i+1/2},t_{n+1}). \tag{4.4}$$

This is defined only when $\Sigma_{i+1/2}$ does not intersect the t axis at times $t > t_n$.

The partition $\{x_1, x_{3/2}, x_{5/2}, \ldots, x_{E-1/2}, x_E\}$ induces a partition of Ω into subregions $\{\Omega^1, \Omega^2, \ldots, \Omega^E\}$, if for each $i = 2,\ldots,E, \Omega^i$ is defined as the subregion of Ω limited by the curves $\Sigma_{i-1/2}$ and $\Sigma_{i+1/2}$, while Ω^1 is that part of Ω which lies to the left of $\Sigma_{3/2}$ and Ω^E is the subregion of Ω which lies to right of $\Sigma_{E-1/2}$ (see Fig. 1). More precisely,

$$\Omega^i = \{(x,t) \in \Omega \mid X(t;x_{i-1/2},t_{n+1}) < x < X(t;x_{i+1/2},t_{n+1})\}, \quad i = 2,\ldots,E-1, \tag{4.5a}$$

$$\Omega^1 = \{(x,t) \in \Omega \mid x < X(t;x_{3/2},t_{n+1})\},$$

and

$$\Omega^E = \{(x,t) \in \Omega \mid X(t;x_{E-1/2},t_{n+1}) < x\}. \tag{4.5c}$$

In view of Eq. (3.16), it is clear that any function which is constant in a subregion of Ω satisfies the adjoint differential equation there. Because of the simplicity of such functions, it is tempting to develop a method of solution using them as test functions. In particular, we consider the system of weighting functions $w^\alpha(x,t), \alpha = 2,\ldots,E-1$, such that for each α, w^α is the characteristic function of Ω^α, i.e.,

$$w^\alpha(x,t) = \begin{cases} 1 & \text{if } (x,t) \in \Omega^\alpha \\ 0 & \text{if } (x,t) \notin \Omega^\alpha, \end{cases} \tag{4.6}$$

$\alpha = 2,\ldots,E-1$. Applying Eqs. (3.21) and (3.22), with any such w^α, it is seen that $\mathcal{K}(w,u) \equiv 0$ except at $\Sigma_{\alpha-1/2}$ and $\Sigma_{\alpha+1/2}$. Furthermore, using the fact that $V_\Sigma \equiv V$, one gets $\mathcal{K}^0(w,u) \equiv 0$, so that

$$\mathcal{K}(w,u) \equiv \mathcal{K}^1(w,u) = \pm(1+V^2)^{-1/2} D\frac{\partial u}{\partial x} \quad \text{on } \Sigma_{\alpha\pm1/2}. \tag{4.7}$$

For any $\alpha = 2,\ldots,E-1, \Omega^\alpha$ does not intersect the lateral boundary $x = l$, because it has been assumed that $V > 0$ and $V_\Sigma = V$ (Fig. 2). If in addition, Ω^α does not intersect the boundary $x = 0$, then $\mathcal{C}(w,u)$ vanishes everywhere, except at the interval of $\partial_{n+1}\Omega$ (i.e., $t = t_{n+1}$), where $x_{\alpha-1} < x < x_{\alpha+1}$. There, $\mathcal{C}(w,u) = -u$. Taking all this into account, the variational principle (3.11b) becomes

$$\int_{x_{\alpha-1}}^{x_{\alpha+1}} u^{n+1}dx + \int_{t_n}^{t_{n+1}} \left(D\frac{\partial u}{\partial x}\right)_{\Sigma_{\alpha+1/2}} dt - \int_{t_n}^{t_{n+1}} \left(D\frac{\partial u}{\partial x}\right)_{\Sigma_{\alpha-1/2}} dt = \int_{x^*_{\alpha-1}}^{x^*_{\alpha+1}} u^n\,dx.$$

Equation (4.8) and a modified version of it designed to incorporate terms contributed by the boundary when Ω^α intersects the time axis will be the starting point of our numerical treatment. Observe that

$$\int_{x_{\alpha-1}}^{x_{\alpha+1}} u^{n+1}\,dx - \int_{x^*_{\alpha-1}}^{x^*_{\alpha+1}} u^n\,dx = O(hk) \tag{4.9a}$$

and

$$\int_{t_n}^{t_{n+1}} \left(D\frac{\partial u}{\partial x}\right)_{\Sigma_{\alpha+1/2}} dt - \int_{t_n}^{t_{n+1}} \left(D\frac{\partial u}{\partial x}\right)_{\Sigma_{\alpha-1/2}} dt = O(hk), \tag{4.9b}$$

where $h = \max(h_{i+1/2}, h_{i-1/2})$ and $k = (t_{n+1} - t_n)$. When h and k are of the same order, $O(hk) = O(h^2) = O(k^2)$. Thus in later developments it will be generally required that integrals such as those appearing in Eqs. (4.9) be evaluated to a precision of $O(hk^2)$, at least. It will be assumed that $h \approx k$, so that $O(hk^2) = O(h^2k)$.

Equations (4.9) *supply information about the sought solution in the interval* $[x_{\alpha-1/2}, x_{\alpha+1/2}]$ *at time* t_{n+1} *and about its x derivative on the characteristics* $\Sigma_{\alpha-1/2}$ *and* $\Sigma_{\alpha+1/2}$. Our goal will be to concentrate all the information on the value of the solution at the "cell center" x_α, at time $t = t_{n+1}$. To this end, in Eq. (4.8), the integrals from t_n to t_{n+1} will be approximated in a fully implicit manner (i.e., by a one-step backward Euler approximation at t_{n+1}). This yields

$$\int_{t_n}^{t_{n+1}} \left\{\left(D\frac{\partial u}{\partial x}\right)_{\Sigma_{\alpha+1/2}} - \left(D\frac{\partial u}{\partial x}\right)_{\Sigma_{\alpha-1/2}}\right\} dt = \left\{\left(D\frac{\partial u^{n+1}}{\partial x}\right)_{\alpha+1/2} - \left(D\frac{\partial u^{n+1}}{\partial x}\right)_{\alpha-1/2}\right\} k + O(hk^2). \tag{4.10}$$

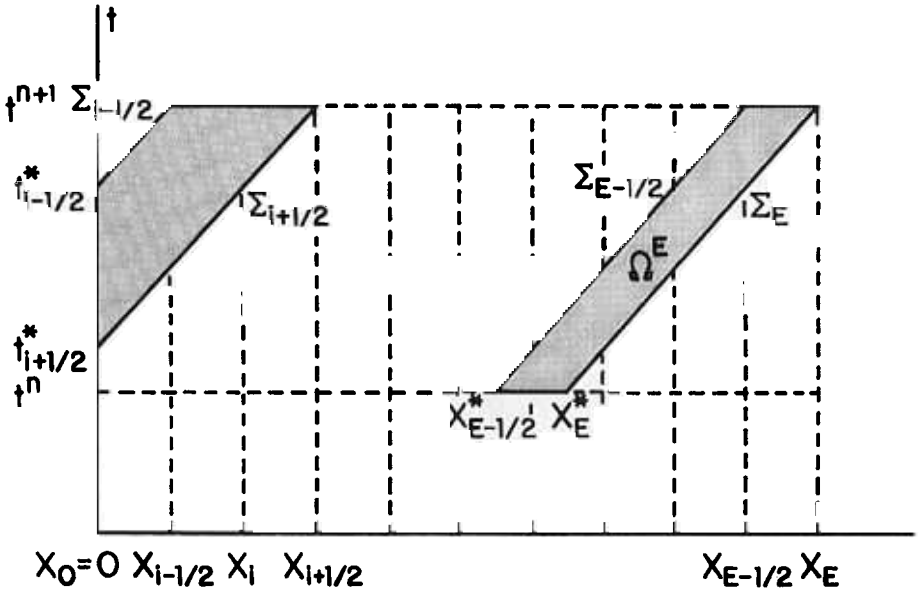

FIG. 2. Case when the domain of test functions intersect the lateral boundaries.

For uniform spacing and constant coefficients, a central difference approximation scheme is applied, which yields

$$\left\{\left(\frac{\partial u^{n+1}}{\partial x}\right)_{\alpha+1/2} - \left(\frac{\partial u^{n+1}}{\partial x}\right)_{\alpha-1/2}\right\}k = \frac{u_{\alpha+1} + u_{\alpha-1} - 2u_\alpha}{h}k + O(h^3 k). \tag{4.11}$$

The extension of this formula to the case of a nonuniform partition can be done in a similar manner. However, such an approximation is only $O(h^2)$ and the overall error in (4.11) becomes $O(h^2 k)$.

In characteristic methods, most of the numerical diffusion is due to the interpolations in space, which are required because, in general, characteristics do not cross the time levels of the time discretization at nodes. To improve this situation, all the approximations in space will be carried out with special care. A special feature of the approximations to be used is that no assumption is made on the shape of the solution.

The first integral in (4.9a) is approximated by

$$\int_{x_{\alpha-1}}^{x_{\alpha+1}} u^{n+1}\,dx = u_\alpha^{n+1} h_\alpha + \frac{1}{24}\left(\frac{\partial^2 u^{n+1}}{\partial x^2}\right)_\alpha h_\alpha^3 + O(h^5) \tag{4.12}$$

and only the second-order derivative requires a numerical approximation, since the information is being concentrated in the cell centers. To get a tridiagonal structure for the matrix, it is convenient to use three-point approximations only. In the case of a "uniform partition," a central difference approximation yields

$$\int_{x_{\alpha-1}}^{x_{\alpha+1}} u^{n+1}\,dx = \left(\frac{u_{\alpha+1} + u_{\alpha-1} + 22u_\alpha}{24}\right)h + O(h^5). \tag{4.13}$$

If the partition is nonuniform, the approximation to the second-order derivative by a three-point scheme is only first order, and the error in the evaluation of the integral in (4.13) is only order four.

The second integral in (4.9a) is approximated using an approach similar to (4.12), i.e., integrating the Taylor expansion of u^n around the midpoint of the interval $[x^*_{\alpha-1}, x^*_{\alpha+1}]$. However, since such point is not a cell center, u^n is not known there and an interpolation must be used to evaluate it. Using three-point formulas, u^n and its second-order derivative can be evaluated to orders three and one, respectively. This permits computing the last integral in Eq. (4.9a) to order four in h.

V. BOUNDARY CONDITIONS

The numerical approximations presented thus far apply only when the subregion $\Omega^\alpha \subset \Omega$ does not intersect the lateral boundaries $\partial_0\Omega \cup \partial_l\Omega$, of the region Ω. When this is not the case, boundary conditions must be included. This section is devoted to presenting procedures for dealing with them.

A. Dirichlet Conditions

For this case, we use $E - 2$ test functions, namely, those associated with subregions $\Omega^2, \ldots, \Omega^{E-1}$. In particular, no test function is applied on the first subregion (Ω^1) or on the last one (Ω^E). See Fig. 2.

1. Inflow Boundary

Dirichlet boundary conditions are incorporated in the numerical equations in two manners: directly, through the boundary terms and indirectly, imposing the condition that, in the numerical approximations, some of the variables take the prescribed boundary values.

Assume Ω^α intersects the inflow boundary, as illustrated in Fig. 2. Then

$$\mathcal{L}u\,d\sigma = \int_{x_{\alpha-1/2}}^{x_{\alpha+1/2}} u^{n+1}\,dx - \int_{t^*_{\alpha-1/2}}^{t_{n+1}} \left\{ \left(D\frac{\partial u}{\partial x}\right)_{\Sigma_{\alpha+1/2}} \quad \left(D\frac{\partial u}{\partial x}\right)_{\Sigma_{\alpha-1/2}} \right\} dt$$
$$- \int_{t^*_{\alpha+1/2}}^{t^*_{\alpha-1/2}} \left\{ \left(D\frac{\partial u}{\partial x}\right)_{\Sigma_{\alpha+1/2}} \quad \left(D\frac{\partial u}{\partial x}\right)_{x=0} \right\} dt - \int_{t^*_{\alpha+1/2}}^{t^*_{\alpha-1/2}} Vu(0,t)\,dt\,. \qquad (5.1)$$

The first two integrals on the right-hand side are similar to those appearing in Eq. (4.8) and can be handled in the same manner as in Sec. IV. In addition, the last one in this equation is easy to deal with, since $u(0,t)$ is the prescribed boundary value. The third integral, however, requires special treatment.

First, observe that

$$\left(D\frac{\partial u}{\partial x}\right)_{\Sigma_{\alpha+1/2}} - \left(D\frac{\partial u}{\partial x}\right)_{x=0} = O(h)\,.$$

Thus, for any $x \in [x_{\alpha-1/2}, x_{\alpha+1/2}]$, one has

$$\left(D\frac{\partial u}{\partial x}\right)(x_{\Sigma_{\alpha+1/2}}(t^*), t^*) - \left(D\frac{\partial u}{\partial x}\right)(0,t^*) = D\frac{\partial u^{n+1}}{\partial x}(x_{\alpha+1/2}) - D\frac{\partial u^{n+1}}{\partial x}(x) + O(hk)\,, \qquad (5.2)$$

where, for brevity, we have written t^* instead of $t^*(x)$. The approximation implied by Eq. (5.2) has the property that the values of the functions involved, at time t^*, are approximated by their values at time t_{n+1}, on the same characteristic. In this manner, crossing of characteristics is avoided. Such a property is important in order to preserve the advantages of characteristic methods.

Equation (5.2) can be used to obtain

$$\int_{t^*_{\alpha+1/2}}^{t^*_{\alpha-1/2}} \left\{ \left(D\frac{\partial u}{\partial x}\right)_{\Sigma_{\alpha+1/2}} \quad \left(D\frac{\partial u}{\partial x}\right)_{x=0} \right\} dt = \left(t^*_{\alpha-1/2} - t^*_{\alpha+1/2}\right)\left(D\frac{\partial u^{n+1}}{\partial x}\right)_{\alpha+1/2}$$
$$+ \int_{x_{\alpha-1/2}}^{x_{\alpha+1/2}} D\frac{\partial u^{n+1}}{\partial x}(x)\frac{dt^*}{dx}(x)\,dx + O(hk^2)\,. \qquad (5.3)$$

As an illustration of the numerical implementation for this equation, we explain the case of constant coefficients. In this case

$$t^*(x) = t_{n+1} - \frac{x}{V} \qquad (5.4)$$

so that

$$\frac{dt^*}{dx} = -\frac{1}{V} \qquad (5.5)$$

and Eq. (5.3) becomes

$$\int_{t^*_{\alpha+1/2}}^{t^*_{\alpha-1/2}} \left\{ \left(D\frac{\partial u}{\partial x} \right)_{\Sigma_{\alpha+1/2}} - \left(D\frac{\partial u}{\partial x} \right)_{x=0} \right\} dt = \frac{x_{\alpha+1/2} - x_{\alpha-1/2}}{V} \left(D\frac{\partial u^{n+1}}{\partial x} \right)_{\alpha+1/2} - \frac{D}{V}\left(u^{n+1}_{\alpha+1/2} - u^{n+1}_{\alpha-1/2} \right) + O(hk^2)$$

In Eq. (5.6), the derivative $\partial u^{n+1}/\partial x$ at $x_{\alpha+1/2}$ $(\alpha = 2, \ldots, E-1)$ must be approximated to order $O(h^2)$ to be consistent with the order of approximation. For a nonuniform mesh, this requires a three-point scheme.

For $\alpha = 2$, the boundary value u_1^{n+1} occurs in equations such as (4.11) and (4.13), and it must be required that at each time level u_1^{n+1} be equal to the prescribed boundary value. This is the indirect manner of imposing the boundary conditions that we referred to at the beginning of this section.

2. Outflow Boundary

Observe that the last test function to be applied is w^{E-1}. The support of this test function is Ω^{E-1}, which does not intersect the lateral boundary $x = l$. Thus, none of the boundary terms involving the outflow boundary occur in the numerical equations and the prescribed boundary values are incorporated in the numerical equations in an indirect manner exclusively, imposing the condition u_E^{n+1} in approximations such as (4.11) and (4.13).

B. Flux Conditions

For this case, we use E test functions. Thus the test functions associated with regions Ω^1 and Ω^E, which were omitted when dealing with Dirichlet boundary conditions, are applied when dealing with this kind of boundary condition, and the values of u^{n+1} at zero and at l are treated as unknowns.

1. Inflow Boundary

Figure 2 illustrates a case in which Ω^α intersects the inflow boundary. For flux boundary conditions, it is more convenient to write Eq. (5.1) in the form

$$\int_{\Omega^\alpha} \mathcal{L}u \, d\sigma = \int_{x_{\alpha-1/2}}^{x_{\alpha+1/2}} u^{n+1} \, dx - \int_{t^*_{\alpha-1/2}}^{t_{n+1}} \left\{ \left(D\frac{\partial u}{\partial x} \right)_{\Sigma_{\alpha+1/2}} - \left(D\frac{\partial u}{\partial x} \right)_{\Sigma_{\alpha-1/2}} \right\} dt - \int_{t^*_{\alpha+1/2}}^{t^*_{\alpha-1/2}} \left(D\frac{\partial u}{\partial x} \right)_{\Sigma_{\alpha+1/2}} dt - \int_{t^*_{\alpha+1/2}}^{t^*_{\alpha-1/2}} F(t) \, dt$$

Here,

$$F \equiv \left(Vu - D\frac{\partial u}{\partial x} \right)_{x=0}$$

is prescribed.

Since $F(t)$ is a datum, the corresponding integral offers no special difficulty in being approximated to any desired order of accuracy. The other integrals can be treated in a

manner similar to what was done in the case of Dirichlet conditions. The approximation

$$\int_{t^*_{\alpha+1/2}}^{t^*_{\alpha-1/2}} \left(D\frac{\partial u}{\partial x}\right)_{\Sigma_{\alpha+1/2}} dt \cong \left(t^*_{\alpha-1/2} - t^*_{\alpha+1/2}\right)\left(D\frac{\partial u^{n+1}}{\partial x}\right)_{\alpha+1/2}$$

is similar to one used in (5.3). However, the term $(D\frac{\partial u}{\partial x})_{x=0}$ which appears in Eq. (5.3), is missing here, because it was incorporated in the flux F. Due to this fact, approximation (5.8) is only $O(k^2)$, which is not consistent with the order of approximation that has been used in all other terms.

However, such a shortcoming was not manifested in the numerical results that were obtained using Eq. (5.8). In all our numerical experiments this approximation was used, since the development of an algorithm fully consistent with the order of accuracy that was set at the beginning of our discussion would require a procedure considerably more elaborate.

In addition, it must be mentioned that when the support of a weighting function intersects any of the corners of the domain Ω, the treatment presented requires slight modifications, whose details we leave out. At the inflow boundary, this happens for two test functions. One is w^1 and there is one more, whose support intersects the corner $(0, t_n)$, as shown in Fig. 2.

2. Outflow Boundary

The only weighting function whose support intersects the outflow boundary is w^E. Applying it, we get

$$\int_{\Omega^E} \mathcal{L}u\, d\sigma = \int_{x_{E-1/2}}^{l} u^{n+1}\, dx - \int_{x^*_{E-1/2}}^{l} u^n\, dx - \int_{t_n}^{t_{n+1}} F(t)\, dt + \int_{t_n}^{t_{n+1}} \left(D\frac{\partial u}{\partial x}\right)_{\Sigma_{E-1/2}} dt. \qquad (5.9)$$

Using three-point approximations, one can evaluate the first two integrals of the right-hand side of this equation to $O(h^4)$. The third one offers no difficulty, since $F(t)$ are data. Finally, an approximating procedure analogous to Eq. (5.8) can be applied to the last integral. However, the comments that were made immediately after Eq. (5.8) hold here too.

VI. NUMERICAL RESULTS

To test the efficiency of the procedure, comparisons with the bilinear version of the ELLAM (BELLAM) were carried out. To be in a better position to do the comparison, the same examples as in [10], which include significant boundary behavior, were solved. They are described next. For the purpose of comparison, it is convenient to take, as we do in this section, $\Omega_x = [a, b]$, instead of $[0, l]$, which was used in the theoretical discussions.

We consider an advancing Gaussian hill that may cross an inflow or outflow boundary. Its general expression is

$$u_a(x,t) = \frac{1}{(1 + 4\pi Dt)^{1/2}} \exp\left(\frac{-\pi(x - Vt)^2}{1 + 4\pi Dt}\right)$$

and the initial and boundary conditions are chosen in such a way that the exact solution of the problem is (6.1). Thus the initial conditions are

$$u_I(x) = \exp(-\pi x^2) \tag{6.2}$$

while the boundary conditions are

$$u(a,t) = u_a(a,t) \tag{6.3a}$$

and

$$u(b,t) = u_a(b,t)$$

whenever Dirichlet conditions are considered. In addition, they are

$$\left(Vu - D\frac{\partial u}{\partial x}\right)(a,t) = \left(Vu_a - D\frac{\partial u_a}{\partial x}\right)(a,t) \tag{6.4a}$$

and

$$\left(Vu - D\frac{\partial u}{\partial x}\right)(b,t) = \left(Vu_a - D\frac{\partial u_a}{\partial x}\right)(b,t) \tag{6.4b}$$

whenever flux boundary conditions are considered. In the numerical examples, only Dirichlet and flux boundary conditions were treated.

Several combinations of initial and boundary conditions are prescribed for Eq. (3.1), but in such a manner that for any of them the exact solution is given by Eq. (6.1). Also, domains considered were $\mathrm{I} = [\frac{7}{3}, 9]$, $\mathrm{O} = [-3, \frac{7}{3}]$, and $\mathrm{N} = [-3, 9]$, with which the pulse crosses an inflow boundary, an outflow boundary, and neither, respectively.

A. Comparison Based on the Euclidean Norm

As explained in previous sections, in the method presented in this article, the information about the sought solution was concentrated in the cell centers at time t_{n+1} exclusively, and no base functions were used. This implies that no assumptions were made about the shape of the solution. This is in contrast with previous ELLAM work, in which shape functions were assumed [10, 21].

One consequence of this way of handling the information is that some of the standard procedures for measuring the errors of approximate solutions are not appropriate. In [10], for example, in which bilinear base functions were used (the space of such functions, which are piecewise linear and continuous in Ω_x, will be denoted by $\mathcal{S}$), the L^2 error of the approximate solution that BELLAM yields (and such approximate solution necessarily belongs to $\mathcal{S}$), was compared with the L^2 error of the projection of the exact solution on $\mathcal{S}$. This ratio is necessarily greater or equal to 1, because of the minimal property of the projection.

When all the information is concentrated at the cell centers, the best we can do is to obtain the exact values at those points. This, however, does not define a function of the space $\mathcal{S}$, and a direct comparison using the L^2 norm is not possible. Of course, one could try to use linear interpolation of the approximate values at the cell centers to associate an element of $\mathcal{S}$ to the approximate solution. However, if one proceeds in that manner, even the optimal solution (i.e., that whose values at the cell centers are the exact values) would give an L^2 error that in general will be greater than that of the projection, again because of the minimal property of the projection. To illustrate this fact and its importance in the different cases tested, Table I compares the L^2 error of the linear interpolation, when the

TABLE I. Comparison of L^2 errors between the projection of the exact solution on the space of piecewise linear functions and the function of this space, whose values are exact at the nodes ("interpolation").

Domain	Δx	Error	
		Projection	Interpolation
N	0.267	0.715E-02	0.159E-01
N	0.053	0.265E-03	0.646E-03
I	0.267	0.715E-02	0.159E-01
I	0.053	0.265E-03	0.646E-03
O	0.267	0.497E-02	0.102E-01
O	0.053	0.177E-03	0.429E-03

values at the cell centers are the exact ones, with the error of the projection of the exact solution, on $\mathcal{S}$. It can be seen that in all cases, the L^2 error of the linear interpolation of the exact values is at least twice that of the projection on $\mathcal{S}$. Thus, if this measure of the error is used, one would not be able to discriminate between different methods on the basis of performance.

Before leaving this point, we would like to remark that when the information about the exact solution consists of the exact values at the cell centers, the extension of this information to the entire interval can be done in manners which are more efficient than using linear interpolation. For example, one could use a high-order interpolation procedure, or solve a local problem (this is a kind of postprocessing), to mention just a few of the possibilities for processing such information.

Therefore a norm that directly compares the values at the cell centers was used to compare the errors of the different methods. The norm chosen was the "average Euclidean norm"

$$\|u - \hat{u}\| = \left(\frac{1}{E} \sum_{1}^{E} (u_i - \hat{u}_i)^2 \right)^{1/2}$$

Here, u_i are the values of the exact solution at the cell centers, while $\hat{u}_i$ are those of the approximate one.

Table II summarizes the numerical results. As in the numerical results of [10], the final time $t_f = 0.5$, Δx is taken to be $\frac{4}{15} \simeq 0.267$ ($Pe = \frac{80}{3}$) and $\Delta x = \frac{4}{75} \simeq 0.0533$ ($Pe = \frac{16}{3}$). For $\Delta x = \frac{4}{15}$, $\Delta t = 0.25$ was used ($Cu = \frac{75}{8}$). For $\Delta x = \frac{4}{75}$, the values 0.25, 0.05, and 0.01 of Δt were used, which correspond to $Cu = \frac{375}{8}, \frac{75}{8}$, and $\frac{8}{7}$, respectively. The integrals involving initial or boundary conditions were evaluated using Gauss-Kronrod rules to a high degree of precision. In Table II, the Euclidean errors associated with the approximate solutions that were derived using ELLAM cells are compared with those obtained when bilinear ELLAM [10] is used. In all cases the errors listed correspond to the final time $t_f = 0.5$.

In general terms, one may conclude that ELLAM cells performed in these examples slightly better than bilinear ELLAM, with respect to the Euclidean error. Runs 1–4 do not involve significant boundary contributions. When this is the case, bilinear ELLAM and the modified method of characteristics (MMOC) become identical [10]. From the results shown in Table II, it follows that in the example treated, ELLAM cells is slightly more precise than MMOC. On the other hand, when the boundary contributions are important, MMOC is considerably less accurate than bilinear ELLAM [10].

TABLE II. Comparison of errors between ELLAM cells and bilineal ELLAM.

		Bound Cond.				Euclidean Error		Maximum Value		
Run	DOM	IN	OUT	Δx	Δt	Cells	Bilinear	Cells	Bilinear	Exact
9	I	F	F	0.267	0.25	0.302E-02	0.684E-02	0.791	0.807	0.784
10	I	F	F	0.053	0.25	0.275E-02	0.287E-02	0.793	0.793	0.784
11	I	F	F	0.053	0.05	0.718E-03	0.821E-03	0.786	0.786	0.784
12	I	F	F	0.053	0.01	0.247E-03	0.293E-03	0.784	0.785	0.784
13	O	D	D	0.267	0.25	0.298E-02	0.452E-02	0.816	0.816	0.816
14	O	D	D	0.053	0.25	0.258E-02	0.262E-02	0.816	0.816	0.816
15	O	D	D	0.053	0.05	0.557E-03	0.614E-03	0.816	0.816	0.816
16	O	D	D	0.053	0.01	0.264E-03	0.202E-03	0.816	0.816	0.816

B. Comparison Based on the Maximum Value

In [10], the maximum of the numerical solution was compared with the maximum of the exact solution. Thus, for completeness, the same comparison was made in this paper and the results are also illustrated in Table II. Inspecting this table, it is also seen that when the performance is judged according to this criterium, the results obtained with ELLAM cells were at least as good as bilinear ELLAM.

Observe that when the domain is $O = [-3, \frac{7}{3}]$, the maximum of the Gaussian distribution (6.1) has already crossed the outflow boundary of the spatial domain, so that when the boundary conditions are of Dirichlet type, the maximum values of the approximate and the exact solutions are equal. Hence, this comparison is not informative in those cases.

VII. CONCLUSIONS

Evidence is presented which indicates that the method introduced here (ELLAM cells) is at least as accurate as bilinear ELLAM (BELLAM) when applied to advection-dominated transport, but easier to implement and more general, since the test functions used (piecewise constant) can also be applied when the equations have nonconstant coefficients.

From a more general perspective, the results of this article illustrate some of the advantages of an approach for developing algorithms to treat numerically partial differential equations that the authors are advocating [4, 11–13], and whose basic ingredients consist of (a) identifying the information about the sought solution contained in the approximate one; and (b) using this insight to choose the interpolation procedure.

In this respect, the results presented indicate that in the problem treated here, there are definite advantages in proceeding in this manner. In particular, many of the problems that were encountered in the construction of FVELLAM [21] were overcome.

The authors wish to thank Agustín Galindo for his participation in the numerical computations presented in the paper, and Thomas F. Russell for having made available the code used in [10]. The work presented in this article was carried out at the Institute of Geophysics of the National University of Mexico (UNAM).

References

1. I. Herrera, in *Computational Methods in Geosciences,* W. E. Fitzgibbon and M. F. Wheeler, Eds., SIAM, Philadelphia, 1992, Chap. 6, p. 66.
2. I. Herrera, in *Computational Methods in Surface Hydrology,* G. Gambolati, A. Rinaldo, and C. A. Brebbia, Eds., Springer-Verlag, Berlin, 1990, p. 433.
3. I. Herrera, in *Computational Methods in Water Resources IX, Vol. I: Numerical Methods in Water Resources,* Computational Mechanics Publications, Southampton, 1992, p. 9.
4. I. Herrera, in *Advances in Computer Methods for Partial Differential Equations VII,* R. Vichnevetsky *et al.,* Eds., International Association for Mathematics and Computers in Simulation (IMACS), New Brunswick, 1992, p. 342
5. I. Herrera, "Unified approach to numerical methods. Part 1. Green's formulas for operators in discontinuous fields," *J. Numer. Methods Partial Different. Equations* **1**, 12 (1985).
6. I. Herrera, L. Chargoy, and G. Alduncin, "Unified approach to numerical methods. Part 3. Finite differences and ordinary differential equations," *J. Numer. Methods Partial Different. Equations* **1**, 241 (1985).
7. I. Herrera, "The algebraic theory approach for ordinary differential equations: Highly accurate finite differences," *J. Numer. Methods Partial Different. Equations* **3**, 199 (1987).

8. I. Herrera, "Solution of general differential equations using the algebraic theory approach," *J. Numer. Methods Partial Different. Equations* **3**, 117 (1987).
9. M. A. Celia, I. Herrera, I. E. Bouloutas, and J. S. Kindred, "A new numerical approach for the advective diffusive transport equations," *Numer. Methods Partial Different. Equations* **5**, 203 (1989).
10. M. A. Celia, T. F. Russell, I. Herrera, and R. Ewing, "An Eulerian-Lagrangian localized adjoint method for the advection-diffusion equation," *Adv. Water Resourc.* **13**, 187 (1990).
11. I. Herrera, R. E. Ewing, M. A. Celia, and T. F. Russell, "Eulerian-Lagrangian localized adjoint method: The theoretical framework," *Numer. Methods Partial Different. Equations* **9**, 431 (1993).
12. G. S. Herrera, "Tratamiento numérico de transporte dominado por advección," M.S. Thesis, Instituto de Geofísica, UNAM, Mexico, 1992.
13. G. S. Herrera, I. Herrera, and A. Galindo, in *Advances in Computer Methods for Partial Differential Equations VII* (Ref. [4]), p. 333.
14. S. P. Neuman, "A Eulerian-Lagrangian numerical scheme for the dispersion-convection equation using conjugate space-time grids," *J. Comput. Phys.* **41**, 270 (1981).
15. S. P. Neuman, "Adaptive Eulerian-Lagrangian finite-element method for advection-dispersion," *Int. J. Numer. Methods Eng.* **20**, 321 (1984).
16. A. O. Garder, D. W. Peaceman, and A. L. Pozzi, "Numerical calculations of multidimensional miscible displacement by the method of characteristics," *Soc. Petrol. Eng. J.* **4**, 26 (1964).
17. L. F. Konikow and J. D. Bredehoeft, "Computer model of two-dimensional solute transport and dispersion in groundwater," *J. Technol. Water Resourc.* Inv. of the U.S. Geol. Surv., Book 7 Chapter C2, 90 p. 1978.
18. J. Douglas, Jr. and T. F. Russell, "Numerical methods for convection-dominated diffusion problems based on combining the method of characteristics with finite element or finite difference procedures," *SIAM J. Numer. Anal.* **19**, 871 (1982).
19. T. F. Russell, M. F. Wheeler, and C. Y. Chiang, in *Mathematical and Computational Methods in Seismic Exploration and Reservoir Modeling*, W. E. Fitzgibbon, Ed., SIAM, Philadelphia, 1986, p. 85.
20. M. S. Espedal and R. E. Ewing, "Characteristic Petrov-Galerkin subdomain methods for two-phase immiscible flow," *Comput. Methods Appl. Mech. Eng.* **64**, 113 (1987).
21. R. W. Healy and T. F. Russell, in *Proceedings of Conference in Solving Ground Water Problems with Models*, J. Lehr, Ed., NWWA, Indianapolis, 1989, p. 483.
22. R. W. Healy and T. F. Russell, "A finite-volume Eulerian-Lagrangian localized adjoint method for solution of the advection-dispersion equation," *Water Resourc. Res.* **29**, 2399 (1993).
23. I. Herrera, *Boundary methods: An Algebraic Theory*, Pitman, Boston, 1984.
24. I. Herrera, in *The Merging of Disciplines: New Directions in Pure, Applied, and Computational Mathematics*, R. E. Ewing, K. I. Gross, and C. F. Martin, Eds., Springer-Verlag, New York, 1986, p. 79.
25. I. Herrera, "On operator extensions: The algebraic theory approach," Proceedings of VII Taller IIMAS-UNAM, Oaxaca, January, 1992.
26. M. B. Allen, I. Herrera, and G. F. Pinder, *Numerical Modeling in Science and Engineering*, Wiley-Interscience, New York, 1988.